Virology 393 (2009) 295–303

Contents lists available at ScienceDirect

Virology

journal homepage: www.elsevier.com/locate/yviro

Overlapping and independent structural roles for human papillomavirus type 16 L2 conserved cysteines

Michael J. Conway [a], Samina Alam [a], Neil D. Christensen [b], Craig Meyers [a,*]

[a] Department of Microbiology and Immunology, The Pennsylvania State University College of Medicine, Hershey, PA 17033, USA
[b] Department of Pathology, The Pennsylvania State University College of Medicine, Hershey, Pennsylvania, PA 17033, USA

ARTICLE INFO

Article history:
Received 9 June 2009
Returned to author for revision 28 July 2009
Accepted 5 August 2009
Available online 5 September 2009

Keywords:
Papillomavirus
Organotypic culture
Assembly
Redox
Capsid

ABSTRACT

Cryoelectron microscopy images of HPV16 pseudovirions (PsV) depict that each pentamer of L1 can be occluded with a monomer of L2. Further research suggests that an N-terminal external loop of L2 exists, which is the target of neutralizing and cross-neutralizing antibodies. Here we show that N-terminal L2 cysteine residues, Cys22 and Cys28, have overlapping and independent structural roles, which affect both early- and late-stage assembly events. Substitution of either cysteine residue enhances infectivity markedly in comparison to wild-type HPV16. However, only Cys22Ser 20-day virions become nearly as stable as wild type. In addition, Cys22Ser, and Cys22,28Ser 20-day virions have lost their susceptibility to neutralization by anti-L2 antibodies, whereas Cys28Ser 20-day virions remain partially susceptible. These results suggest that Cys28 is necessary for late-stage stabilization of capsids, while Cys22 is necessary for proper display of L2 neutralizing epitopes.

Introduction

Human papillomavirus (HPV) virions contain a single, circular dsDNA genome of approximately 8 kb, which associates with histones to form a chromatin-like structure (Conway and Meyers, 2009; Doorbar, 2005; Longworth and Laimins, 2004). This minichromosome is packaged within a nonenveloped, icosahedral capsid composed of 72 pentamers of the major capsid protein L1 and an unknown number of the minor capsid protein L2 (Buck et al., 2008; Conway and Meyers, 2009; Finnen et al., 2003; Trus et al., 1997). High-resolution images of native bovine papillomavirus 1 (BPV1) and HPV16 pseudovirions (PsV) suggest that pentamers of L1 can be occluded with a monomer of the minor capsid protein L2 (Buck et al., 2008; Trus et al., 1997).

Critical to the production of an effective second-generation vaccine, an N-terminal "external loop" of L2 exists, which can be the target of neutralizing and cross-neutralizing antibodies (Conway et al., in press; Day et al., 2008a; Gambhira et al., 2007; Kondo et al., 2007; Liu et al., 1997). Specifically, peptides generated from L2 residues 17–36 have been shown to elicit a wide-ranging cross-neutralizing antibody response (Gambhira et al., 2007). Two N-terminal L2 cysteines, Cys22 and Cys28, are conserved among all mammalian and avian papillomaviruses, and recent work utilizing HPV16 quasivirions (QV) has depicted the presence of a permanent disulfide bond between Cys22 and Cys28—suggestive of the structural relevance of these residues (Campos and Ozbun, 2009). Considering the proximity of Cys22 and Cys28 to the cross-neutralizing 17–36 epitope, we hypothesized that Cys22 and/or Cys28 might play a role in structural rearrangements of L2, which facilitate the presentation of cross-neutralizing epitopes contained within the L2 external loop.

Previously, we have shown that organotypic culture-derived native virions, in the context of the complete papillomavirus life cycle, utilize a tissue-spanning redox gradient, which facilitates multiple redox-dependent assembly and maturation-like events over the course of many days (Conway and Meyers, 2009). We showed that stability and specific infectivity of 20-day virions increases over 10-day virions, that 20-day virions become more susceptible to neutralization than 10-day virions, and that both viral DNA encapsidation and infectivity of HPV-infected tissues are redox-dependent in that they can be manipulated via the treatment of organotypic tissues with oxidized glutathione (GSSG), which is temporally and concentration-dependent (Conway and Meyers, 2009). These data suggest that papillomavirus virions undergo a very long assembly process within tissue, which is dependent on disulfide bond formation.

Here, we show that N-terminal HPV16 L2 cysteine residues, Cys22 and Cys28, have overlapping and independent structural roles, which can be temporally distinguished. In our system, Cys28Ser 10-day and 20-day virions are more physically fragile than wild type, while Cys22Ser 20-day virions become nearly stable as wild type, suggesting that Cys28 is involved in late-stage stabilization of virions. In addition, Cys22Ser and Cys22,28Ser 20-day virions have lost their susceptibility to neutralization by anti-L2 antibodies, whereas Cys28Ser 20-day virions remain susceptible to neutralization. These results suggest that Cys22 plays a major role and Cys28 a minor role in the display of N-terminal cross-neutralizing epitopes.

* Corresponding author. Fax: +1 717 531 4600.
E-mail address: cmm10@psu.edu (C. Meyers).

0042-6822/$ – see front matter © 2009 Elsevier Inc. All rights reserved.
doi:10.1016/j.virol.2009.08.010

In contrast to recent work utilizing HPV16 QV, substitution of either cysteine residue for serine in HPV16 organotypic culture-derived virions enhanced infectivity markedly over wild type (Campos and Ozbun, 2009). In addition, specific infectivity of 20-day mutant virions increased over their 10-day mutant counterparts more than wild type, suggesting that Cys22 and Cys28 both hinder a transitional phase involved in the enhancement of specific infectivity in 20-day wild-type virions (Campos and Ozbun, 2009; Conway and Meyers, 2009).

Results

Establishment of cell lines infected with HPV16 L2 mutants

To develop producer cell lines that can synthesize organotypic culture-derived native virions from differentiating epithelia, primary human foreskin keratinocytes (HFKs) were electroporated with linearized wild-type and site-directed mutagenized HPV16(114/B) DNA (Kirnbauer et al., 1993). The recircularization and maintenance of episomal HPV16 viral genomes for representative HPV16 L2 Cys22Ser, Cys28Ser, and Cys22,28Ser cell lines can be seen in Fig. 1A. Data for wild-type HPV16 cell lines have been published previously (Conway et al., in press; McLaughlin-Drubin, Christensen, and Meyers, 2004). The total number of episomal copies per cell was less in mutant cell lines (~10–200 copies/cell) than the wild-type cell line utilized (>1000 copies/cell). We do not believe that the lower copy numbers observed in the mutant cell lines are significant regarding productivity of tissues as previous reports have suggested that copy number does not directly correlate with the titer of HPV-infected organotypic tissues (McLaughlin-Drubin, Christensen, and Meyers, 2004; McLaughlin-Drubin et al., 2003; Meyers, Mayer, and Ozbun, 1997). In addition, the use of viral genome equivalents (vge) and/or detection of the major capsid protein via Western blot analysis allows for the analysis of the relative specific infectivity (i.e., vge or protein to infectivity ratio) of individual virions produced by HPV-infected organotypic tissues, which eliminates potential differences in tissue productivity (Conway et al., in press). For each mutant genome, multiple episomal DNA-containing cell lines were produced and utilized in experiments to control for PCR fidelity during the mutagenesis protocol. In addition, L2 ORFs were sequenced to verify the existence of the intended mutation and the absence of erroneous mutations in all cases. Stable cell lines were then allowed to grow as stratified and differentiated epithelial tissues in organotypic culture (Fig. 1B).

Infectivity of L2 mutant virions

To determine if substitution of L2 cysteines altered infectivity of crude viral preps (CVPs) or specific infectivity of virions (i.e., vge to infectivity ratio), we performed duplex RT-qPCR-based infectivity assays on 10- and 20-day CVPs made from wild-type and mutant-infected organotypic tissues. All CVPs were benzonase treated to digest nonencapsidated and susceptible viral genomes within the CVP (Conway and Meyers, 2009). The completeness of the benzonase reaction was verified by assessing the digestion of 1 μg of spike HPV16 DNA under identical conditions (data not shown). Surprisingly, Cys22Ser and Cys28Ser CVPs were consistently much more infectious than wild type, with 10-day mutant CVPs averaging 100-fold more E1^E4 expression (Fig. 2A) and 20-day mutant CVPs averaging 10,000- and 1000-fold more E1^E4 expression, respectively (Fig. 2B). Ten- and twenty-day Cys22,28Ser CVPs were more infectious, with 10- and 1,000-fold more E1^E4 expression than wild type, respectively (Figs. 2A, B). These results suggest that either more virions are produced within Cys22Ser, Cys28Ser, and Cys22,28Ser mutant organotypic tissues or each individual mutant virion is more infectious than wild type.

To quantify the total number of vge within each CVP, we utilized a qPCR-based DNA encapsidation assay to detect endonuclease-resistant genomes as described previously and in the Materials and methods section (Conway et al., in press; Holmgren et al., 2005; Wang et al., 2009). Briefly, 10 μl aliquots of CVPs were Hirt extracted for viral nucleic acid and extracted DNA was run alongside a standard curve made from 10-fold dilutions of HPV16 DNA in a SYBR-green-based qPCR reaction. As the total number of viral genomes within each point on the standard curve was known (based on the weight of an individual nucleotide and the size of the HPV16 genome), values obtained from experimental samples were back calculated and converted to total genomes per raft. Because of the low productivity of organotypic culture in producing HPV virions in comparison to techniques that produce HPV virus-like particles (VLPs), pseudovirions (PsV), and quasivirions (QVs), in addition to high background cellular keratin bands during Western blot analyses, vge is the most quantitative method for normalization at this time (Buck et al., 2004; Conway and Meyers, 2009; Pyeon, Lambert, and Ahlquist, 2005). At 10 days, Cys22Ser CVPs contained 4.5% ± 1.3%, Cys28Ser CVPs contained 7.5% ± 1.5%, and Cys22,28Ser CVPs contained 1.6% ± 0.5% of the total number of encapsidated genomes contained within wild-type CVPs, with included standard error values (Fig. 3A). Such decreases in encapsidated genomes found in mutant CVPs suggest that the observed increase in infectivity (Figs. 2A, B) in comparison to wild type is

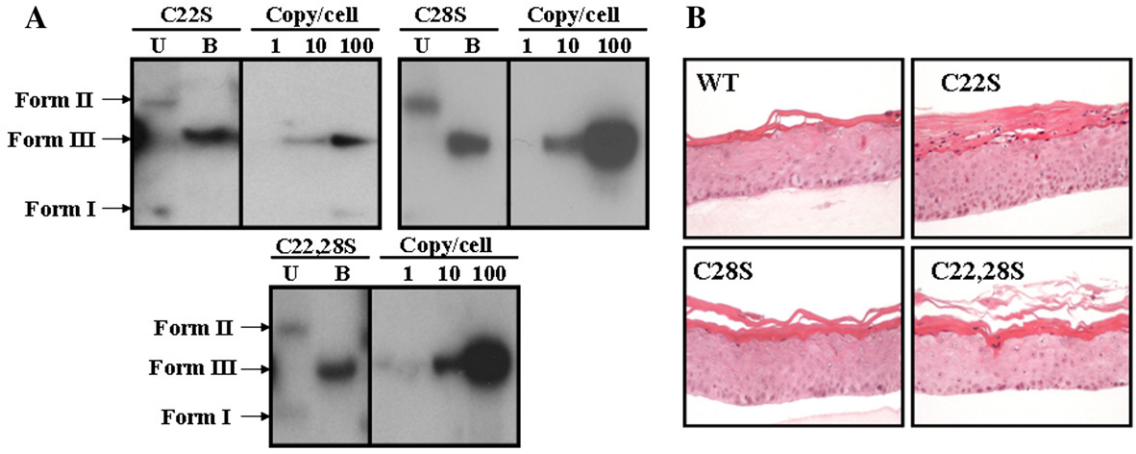

Fig. 1. Episomal maintenance of mutant viral genomes and stratification of organotypic cultures. (A) Southern blot hybridization of HPV16(114/B)-infected HFK cell lines with Cys22Ser, Cys28Ser, and Cys22,28Ser substitutions. Uncut (U) and single *Bam*HI cut (B) episomal genomes are shown in addition to 1, 10, and 100 viral genome copies per 5 μg of total genomic DNA. (B) Hematoxylin and eosin staining of paraffin-embedded, 10-day wild-type (WT), Cys22Ser-, Cys28Ser-, and Cys22,28Ser-infected organotypic tissue.

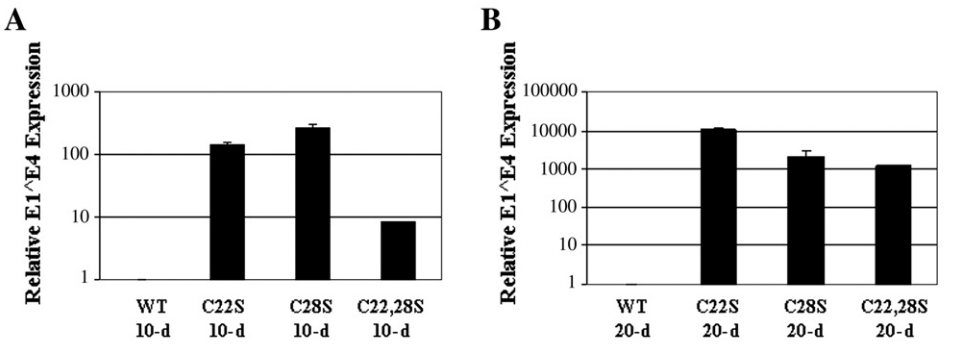

C

Specific Infectivity of Virions (Vge to Infectivity Ratio)

WT 10-d	WT 20-d	C22S 10-d	C22S 20-d	C28S 10-d	C28S 20-d	C22,28S 10-d	C22,28S 20-d
1 ± 0.07	2.2 ± 0.05	2,868 ± 214	27,026 ± 840	3,608 ± 498	43,965 ± 1,525	346 ± 86	128,688 ± 14,000

Fig. 2. (A–B) Relative RT-qPCR-based infectivity analysis of 10- and 20-day wild-type, Cys22Ser, Cys28Ser, and Cys22,28Ser crude viral preps (CVPs) and (C) relative specific infectivity (vge-to-infectivity ratio) of wild-type and mutant virions. Fifty microliters of (A) 10- or (B) 20-day wild-type or mutant CVPs were diluted 1:10 in a total volume of 500 μl HaCaT media and utilized to infect 5×10^5 HaCaT cells. RNA was harvested and relative E1^E4 expression was detected via duplex RT-qPCR and plotted with 10- and 20-day wild-type infections set to 1.0. To calculate specific infectivity of virions (C), vge values obtained in Figs. 3A, B were utilized to normalize RT-qPCR-based infectivity assay data in panels A, B. Ten-day wild-type infections were set to 1.0. Experiments were performed in triplicate with an incorporated ± standard error of the mean.

not due to an increase in total virion number. To support that lower vge yields correlate with the destabilization of capsids, Cys428Ser mutant-infected tissues were generated as described for the L2 mutants above. Substitutions of Cys428 have been shown to be destabilizing in virus-like particles (VLPs), PsV, and organotypic culture-derived virions (Buck et al., 2005; Conway et al., in press; Ishii, Tanaka, and Kanda, 2003; Li et al., 1998). The Cys428Ser mutant stable cell line utilized contained 100 episomal copies/cell and grew into fully stratified and differentiated epithelial tissues (Conway and Meyers, 2009). As 10-day Cys428Ser mutant CVPs contained 1.2% ± 0.3% of the total number of encapsidated genomes contained within wild-type CVPs, it supports that substitution of L2 cysteine residues destabilize papillomavirus particles (Fig. 3A). At 20 days, Cys22Ser CVPs contained 73.0% ± 2.0%, Cys28Ser CVPs contained 4.2% ± 0.76%, and Cys22,28Ser CVPs contained 1.5% ± 0.06% of the total number of encapsidated genomes contained within 20-day wild-type CVPs (Fig. 3B). The dramatic increase in observed encapsidated genomes within 20-day Cys22Ser CVPs and the lack of increase in Cys28Ser and Cys22,28Ser CVPs suggest that either the loss of Cys22 and consequent disulfide bonding stabilizes 20-day virions or Cys28 is critical for late-stage encapsidation of genomes and/or stabilization of capsids via a novel disulfide interaction.

In Fig. 2C, vge values obtained in Figs. 3A, B were utilized to normalize RT-qPCR-based infectivity assay data in Figs. 2A, B. Taking vge into consideration, enhanced specific infectivity was observed for 10-day Cys22Ser, Cys28Ser, and Cys22,28Ser virions, at 2868-, 3608-, and 346-fold more infectious than wild type, respectfully. At 20 days, the specific infectivity of mutant virions all became markedly more infectious than wild type in addition to their 10-day mutant counterparts, with Cys22Ser virions 27,026-fold, Cys28Ser virions 43,965-fold, and Cys22,28Ser virions 128,688-fold more infectious than 10-day wild-type virions. As specific infectivity of 20-day wild-type virions is enhanced, approximately 2.2-fold over 10-day wild-type virions, 20-day Cys22Ser, Cys28Ser, and Cys22,28ser virions were 12,284-, 19,984-, and 58,494-fold more infectious than 20-day wild-type virions.

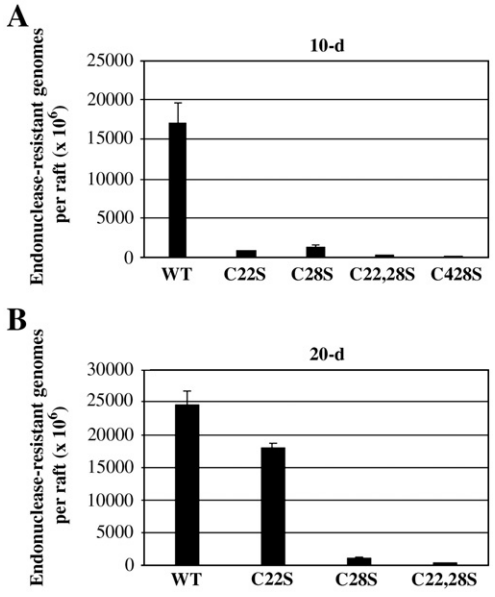

Fig. 3. Encapsidated genomes within benzonase-treated, (A) 10- and (B) 20-day wild-type, Cys22Ser, Cys28Ser, Cys22,28Ser, and Cys428Ser crude viral preps (CVPs). Equal aliquots of three wild-type and mutant CVPs were incubated with Proteinase K and SDS for 2 h, spiked with 6% 2-ME and boiled for 10 min prior to extracting endonuclease resistant genomes. Viral genomes were plotted against a standard curve using SYBR green-based chemistry. All experiments were performed in triplicate with an incorporated standard error of the mean.

Stability of L2 mutant virions

When we performed our DNA encapsidation assay on 10- and 20-day wild-type and mutant CVPs, we did not detect an increase in the amount of endonuclease-resistant genomes in mutant CVPs, which would correlate with their increased infectivity titers (Figs. 3A, B). Instead we detected marked decreases in endonuclease-resistant genomes within mutant CVPs. We interpret these results to mean that either fewer particles are made in mutant tissues or that mutant virions are susceptible to endonuclease digestion and are thus more fragile than wild-type virions. Both explanations suggest that, even though more fragile and less apt to form a proper capsid, virions made with mutant L2 proteins are more infectious than wild type. It is also possible that the cysteine mutations lead to the production of particles that are much more resistant to chemical reduction, which would lead to the lack of detection of endonuclease-resistant genomes in our DNA encapsidation assay.

To further assess the stability of wild-type and mutant virions, we fractionated CVPs on Optiprep step gradients and infected HaCaT cells

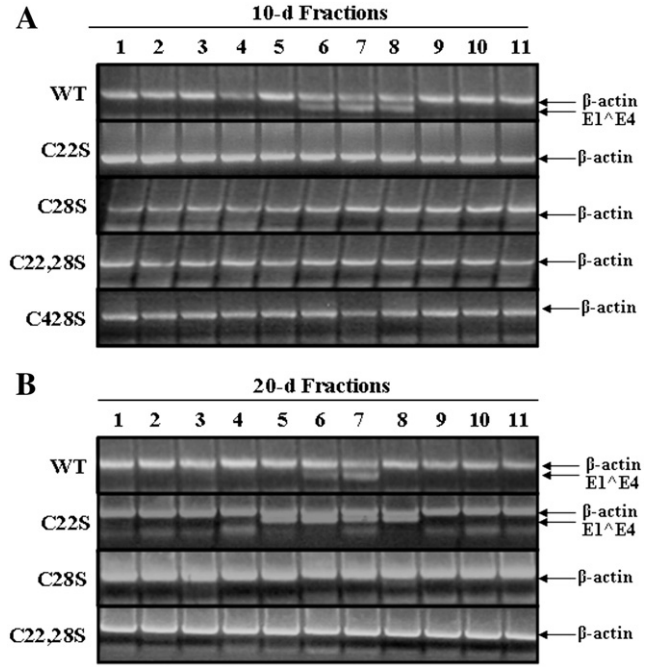

Fig. 4. Stability of (A) 10- and (B) 20-day wild-type, Cys22Ser, Cys28Ser, Cys22,28Ser, and Cys428Ser virions. (A) 10-day, benzonase-treated, wild-type, Cys22Ser, Cys28Ser, Cys22,28Ser, and Cys428ser crude viral preps (CVPs) were Optiprep-fractionated and fractions were inoculated into HaCaT cells at a dilution of 1:10. Fraction 1 represents the top of the gradient, while fraction 11 represents the bottom. Infectivity was assessed via RT-PCR by amplifying E1^E4 in tandem with the PCR control, β-actin. (B) Twenty-day, benzonase-treated, wild-type, Cys22Ser, Cys28Ser, Cys22,28Ser, and Cys428ser crude viral preps (CVPs) were Optiprep fractionated and fractions were inoculated into HaCaT cells at a dilution of 1:10. Fraction 1 represents the top of the gradient, while fraction 11 represents the bottom. Infectivity was assessed via RT-PCR by amplifying E1^E4 in tandem with the PCR control, β-actin.

with 1:20 dilutions of 10-day and 1:1000 dilutions of 20-day fractions to assay for infectivity via RT-PCR (Figs. 4A, B). Optiprep gradient fractionation of HPV virions has been reported to destabilize capsids (Buck et al., 2004; Conway and Meyers, 2009). While infectivity was detected in fractions 6–8 from 10-day wild-type CVPs, infectivity was not detected in any fraction from 10-day mutant CVPs (Fig. 4A). To verify that loss of infectivity was due to fragility of capsids, CVPs made from 10-day organotypic tissues capable of synthesizing the HPV16 L1 mutant, Cys428Ser, were Optiprep fractionated and assayed for infectivity (Ishii, Tanaka, and Kanda, 2003; Li et al., 1998; Sapp et al., 1998) (Fig. 4A). Infectivity was also not observed in Optiprep-fractionated 10-day Cys428Ser CVPs, suggesting that the L2 mutations do perturb the structure of the virion leading to a more fragile phenotype (Fig. 4A). However, like fractions from 20-day wild-type CVPs where infectivity is observed in fractions 6–7, infectivity can be detected in 20-day Cys22Ser CVP fractions 5–8 (Fig. 4B). Along with the DNA encapsidation assay results in Figs. 2A, B, these results suggest that Cys22Ser virions are more fragile than wild type at 10 days but become more stable at 20 days. Cys28Ser and Cys22,28Ser virions remain fragile at both time points, suggesting that Cys28 plays a crucial role in late-stage stability of papillomavirus virions whereas Cys22 plays a role in virion stability at all stages of papillomavirus assembly.

Neutralization of L2 mutant virions with anti-L2 Abs

Because of the proximity of HPV16 N-terminal cysteines to cross-neutralizing epitopes, we sought to determine whether Cys22Ser, Cys28Ser, and Cys22,28Ser mutations would alter the wild-type neutralization profile. Neutralizing activities of anti-HPV16 L2 antisera were measured by inhibition of infection of HaCaT cells with wild-type and mutant HPV16 (Figs. 5A, B) (Gambhira et al., 2007; Kondo et al., 2007).

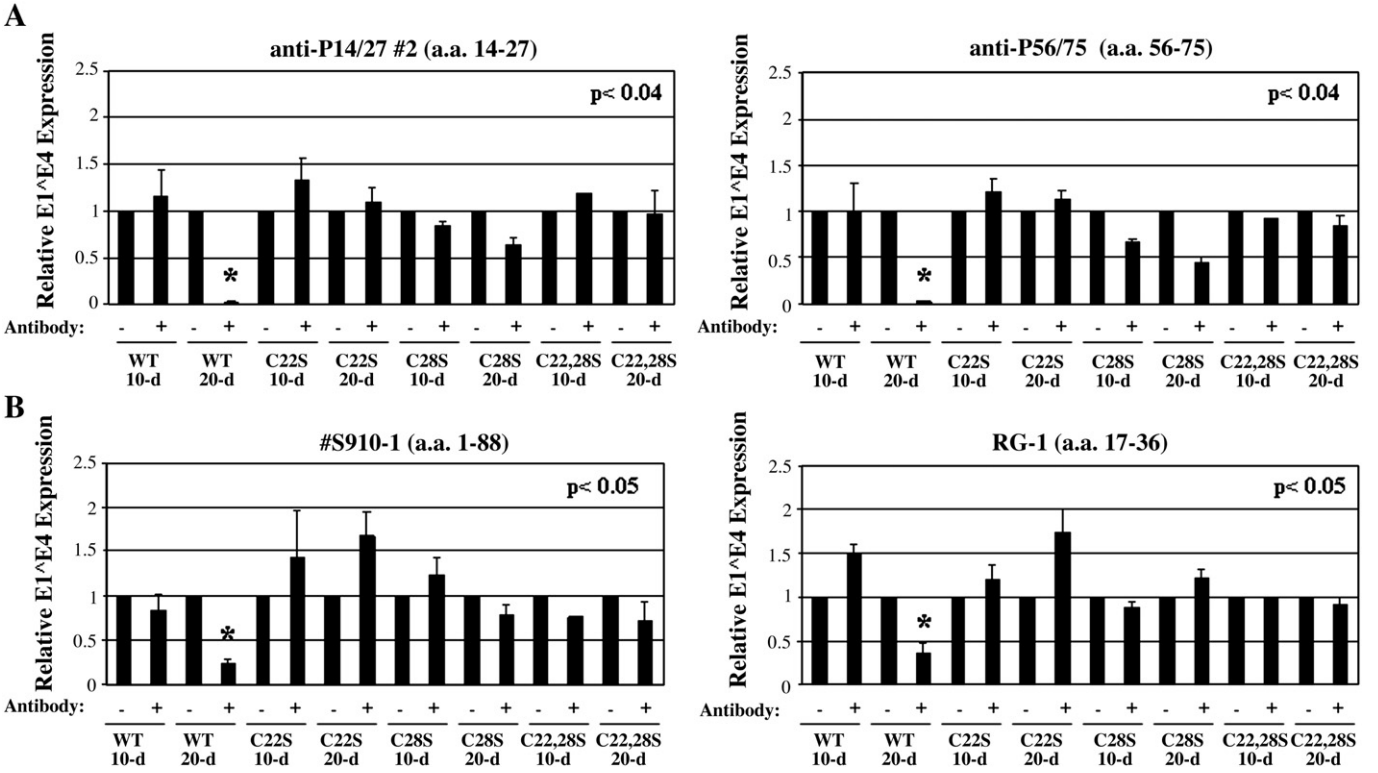

Fig. 5. Neutralization of 10- and 20-day wild-type, Cys22Ser, Cys28Ser, and Cys22,28Ser crude viral preps (CVPs) with (A) anti-L2 "external loop" polyclonal (anti-P14/27 #2 and anti-P56/75) and (B) monoclonal antibodies (S910-1 and RG-1). Fifty microliters of each CVP was diluted 1:10 with (+) or without (−) a 1:100 dilution of each antibody in a total volume of 500 μl of HaCaT media. Neutralization reactions commenced for 1 h at 37 °C prior to infection of 5×10^6 HaCaT cells. RNA was harvested and infectivity was assessed by measuring relative E1^E4 expression via duplex RT-qPCR. No antibody controls (−) were set to 1.0. All experiments were performed in triplicate with an incorporated standard error of the mean.

Antisera were mixed 1:100 with 50 μl of 10- and 20-day wild-type, Cys22Ser, Cys28Ser, and Cys22,28Ser CVPs and then inoculated to HaCaT cells. This concentration of antisera was near the highest concentration tested in previous studies (Gambhira et al., 2007; Kondo et al., 2007). Forty-eight hours later, duplex RT-qPCR-based infectivity assays were utilized to detect relative expression of E1^E4. The vge/cell added for neutralizations of 10-day CVPs is as follows: 34,338 for wild type, 1560 for Cys22Ser, 2,570 for Cys28Ser, and 546 for Cys22,28Ser. The vge/cell added for neutralizations of 20-day CVP is as follows: 49,353 for wild type, 36,034 for Cys22Ser, 2062 for Cys28Ser, and 719 for Cys22,28Ser. The wide range of wild-type and mutant vge/CVP prohibited us from performing the neutralization assay utilizing equal vge numbers. Because of the low productivity of organotypic culture in producing HPV virions, in addition to the severe cross-reactivity between antibodies and cellular keratin, vge remains the most quantitative method for normalization (Conway and Meyers, 2009). As shown in Figs. 5A, B, wild-type HPV16 can only be effectively neutralized with a panel of anti-HPV16 L2 antibodies: anti-P14/27 #2 (AA 14–27), anti-P56/75 #1 (AA 56-75), #S910-1 (AA 1-88), and RG-1 (AA 17-36) when virions have matured within tissue for 20 days (Conway et al., in press; Gambhira et al., 2007; Kondo et al., 2007). Similar to wild type, 10-day Cys22Ser, Cys28Ser, and Cys22,28Ser mutant virions are not effectively neutralized (Figs. 5A, B). Twenty-day Cys22Ser and Cys22,28Ser virions are also not effectively neutralized even when fewer vge/cell are neutralized as compared to wild type (Figs. 5A, B). In addition to the failure of antibodies to neutralize, significant increases in infectivity were observed after addition of #S910-1 to 10- and 20-day Cys22Ser virions and when RG-1 was added to 20-day Cys22Ser virions. In contrast, 20-day Cys28Ser virions partially retained susceptibility to neutralization by anti-P14/27 #2, and anti-P/56/75 #1 as compared to wild-type (Figs. 5A, B). These antibody neutralization studies suggest that Cys22 is important in late-stage exposure of cross-neutralizing epitopes on the L2 external loop. Cys28 appears to play a minor role.

Discussion

While major capsid protein L1 is sufficient to produce virus-like particles (VLPs) in vitro, the minor capsid protein L2 has a growing repertoire of structural and functional roles not limited to DNA encapsidation, assembly, stabilization, entry, and transit of genomes into the nucleus (Bordeaux et al., 2006; Bossis et al., 2005; Buck et al., 2005; Finnen et al., 2003; Ishii et al., 2005; Richards et al., 2006; Zhou et al., 1994). Recent cryoelectron microscopy image reconstructions of HPV16 pseudovirions (PsV) corroborate previous studies that depict L2 localization within the inner conical hollow of L1 pentamers (Buck et al., 2008; Trus et al., 1997). While the general location of L2 within the capsid appears understood, many aspects of the protein are unknown or controversial such as the total number of L2 proteins per virion, detailed structural information about L2 and how it interacts with its neighboring L1 pentamers, and functional aspects regarding L2 structural rearrangements, which allow the L2 external loop to facilitate neutralizing epitope recognition, furin cleavage, and interaction with cellular and extracellular receptors (Day et al., 2008a; Day et al., 2008b; Liu et al., 1997; Richards et al., 2006; Yang et al., 2003).

Many studies have reported domains of L2 that interact with L1 (Buck et al., 2008; Finnen et al., 2003; Lowe et al., 2008; Touze et al., 2000). L2 only appears to interact with capsomeres of L1 and not intact VLPs, suggesting that L2 and L1 co-assemble (Finnen et al., 2003). During differentiation, such co-assembly would require a regulated process mediated by interactions between these two proteins. The C-terminus of both BPV1 and HPV11 L2 has L1 interacting domains, in addition to an internal L1 interacting domain in BPV1 L2 (Touze et al., 2000). Recent research has also concluded that the N-terminus of L2 may interact with L1, although a physical interaction has yet to be validated (Buck et al., 2008; Lowe et al., 2008). Since L2 enhances assembly of L1 capsomeres in the absence of disulfide bonding, hydrophobic interactions between L2 and L1 are most likely to initiate early assembly events (Ishii et al., 2005). In the context of stratified epithelial tissue, these early assembly events would appear to occur in the chemically reducing environment of the suprabasal compartment, which would necessitate hydrophobic rather than disulfide interactions (Conway and Meyers, 2009).

The individual domains of L2 involved in binding to L1 at various time points during the assembly process are not known. However, recent advances in VLP, and PsV technology have found that a maturation step is required for stabilization of synthetic papillomavirus particles to make them appear more native virus-like (Buck et al., 2005; Mach et al., 2006). The morphological change from immature to mature PsV opens the possibility of temporal interactions between L2 and L1 (Buck et al., 2005). Such a maturation step is also evident is organotypic culture-derived native virions as virions extracted from 20-day-old tissues have a higher specific infectivity, are more stable, and become more susceptible to neutralization than virions extracted from 10-day-old tissues (Conway and Meyers, 2009).

Temporal changes in L2 structure have been elucidated through the neutralization of HPV16 PsV with the anti-L2 “external loop” monoclonal antibody RG-1 (AA 17–36) whereby mature PsV are only effectively neutralized by this antibody post-cell adsorption (Day et al., 2008a). Reports have also shown that N and C-terminal L2 epitope tags are not accessible to antibody binding until after hours of cell binding (Day et al., 2004). In addition, it was reported by our laboratory that effective neutralization of HPV16 organotypic culture-derived virions via RG-1 only occurs when virions are extracted from 20-day-old tissue (Conway and Meyers, 2009). These results indicate that L2 conformational changes can occur both during capsid assembly and at the cell surface (Conway et al., in press; Day et al., 2004; Day et al., 2008a; Richards et al., 2006).

Hypothesizing that L2 cysteines may be involved in the externalization of neutralizing and cross-neutralizing epitopes, and perhaps temporal interactions with L1, we substituted each cysteine for serine, making cell lines competent in synthesizing mutant native virions in organotypic culture. Surprisingly, all mutated genomes led to the production of 10- and 20-day virions with a higher specific infectivity than wild-type HPV16. This was in contrast to work with mature HPV16 quasivirions (QV) whereby identical amino acid substitutions led to the production of noninfectious virions (Campos and Ozbun, 2009). This discrepancy may underscore subtle differences in capsid structure between papillomavirus particles produced in monolayer cell culture versus in differentiating epithelial tissue. However, infectivity of the mutant QV was only assessed after Optiprep fractionation rather than from crude 293TT cell lysates (Campos and Ozbun, 2009). In our hands, infectivity of 10-day mutant virions is also lost after Optiprep fractionation and surprisingly restored in 20-day Cys22Ser virions. This suggests that mature QV are as fragile as our 10-day virions. Different virion extraction protocols may also play a role as monolayer culture-derived particles are harvested via detergent lysis, while organotypic culture-derived particles are harvested via salt extraction. We predict that such an increase in specific infectivity of these mutant virions may be due to an enhanced presentation of the N-terminal furin cleavage site or through the induced fragility of the virions which may lead to more effective release of viral genomes post-entry (Day et al., 2008a; Richards et al., 2006).

The proximity of Cys22 and Cys28 to one another might lead to the hypothesis that these residues form a critical disulfide bond with each other. Recent biochemical analyses of mature HPV16 QV attest to a disulfide linkage between Cys22 and Cys28 (Campos and Ozbun, 2009). Our data suggest that a permanent disulfide bond does not exist between Cys22 and Cys28 since differential phenotypes are observed in 20-day mutant virions regarding their stability and susceptibilities to neutralization via anti-L2 neutralizing antibodies. It appears that Cys28Ser and Cys22,28Ser virions are more physically

fragile than wild-type HPV16 at all time points, suggesting that Cys22 is insufficient to stabilize the capsid at 20 days. In contrast, Cys22Ser virions are more physically fragile than wild-type HPV16 at day 10; however, at day 20, Cys22Ser virions regain their stability, suggesting that Cys28 may play a role in late-stage stabilization of the capsid. A scenario can be visualized incorporating previous findings where Cys22 and Cys28 play a role in early stabilization of the capsid, perhaps through a critical disulfide interaction (Campos and Ozbun, 2009). At a later time point, however, Cys22 is dispensable for capsid stabilization and Cys28 becomes critical (Fig. 6). This model suggests that mature QV lack a conformational capsid rearrangement that only occurs in virions derived from fully differentiated epithelial tissue.

The location at which the L2 external loop extrudes from the capsid is, at this point, unknown. Analysis of the inner conical hollow of an HPV16 L1 pentamer depicts a single L1 cysteine residue, which may be in an opportune location to temporally interact with L2 cysteines during capsid assembly and maturation (Chen et al., 2000). While previous examinations into L1–L2 disulfide interactions failed to yield concrete evidence that such bonding occurs, it is tempting to suggest that Cys28 may temporally isomerize with Cys145 during capsid assembly (Doorbar and Gallimore, 1987).

Neutralization studies also suggest that Cys22 and Cys28 may play a role in the architecture of the cross-neutralizing epitope-containing L2 “external loop”. While 20-day wild-type HPV16 virions are efficiently neutralized by many anti-L2 external loop antibodies, 20-day Cys22Ser, and Cys22,28Ser mutant virions are resistant to efficient neutralization, suggesting that their L2 epitopes are not available to these antibodies. Twenty-day Cys28Ser virions remain susceptible to partial neutralization. This result suggests that while Cys22 is not important for stabilization of the capsid at 20 days, it appears to modulate the accessibility of neutralizing epitopes on the L2 external loop.

These genetic and molecular analyses of L2 mutant virions serve to provide a framework for further detailed structural studies of papillomavirus capsid interactions. Since the atomic resolution of L2 from native virions and the L2 “external loop” from L1/L2 HPV16 PsV has not been solved, it is imperative that genetic and biochemical research be performed in tandem in order to elucidate the many roles of L2 in the papillomavirus life cycle.

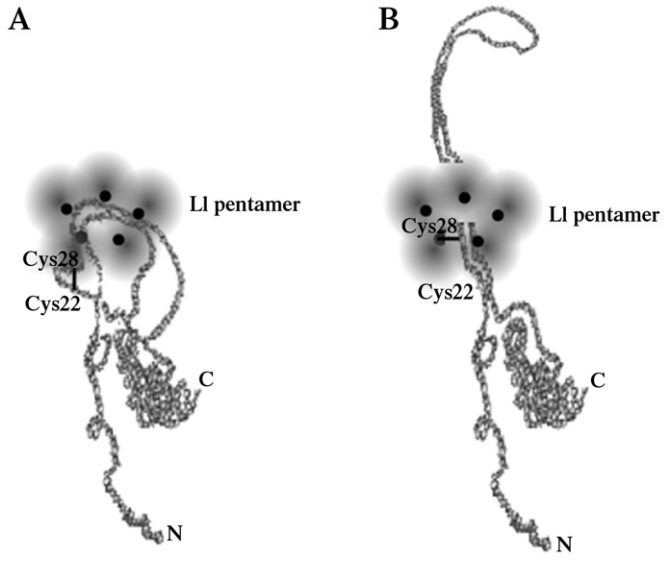

Fig. 6. Hypothetical model of HPV16 L2 externalization through the inner conical hollow of an L1 pentamer. (A) Cys22 and Cys28 are linked via a disulfide bond (black bar) in 10-day native virions forming a hairpin structure. (B) Cys28 and an unknown L1 cysteine residue (black circle) are linked via a disulfide bond (black bar) which stabilizes 20-day capsids.

Materials and methods

Mutagenesis

pBSHPV16(114/B) DNA, a generous gift from M. Dürst, was utilized as a template for site-directed mutagenesis using Strategene's Quikchange II XL Site-Directed Mutagenesis Kit (Kirnbauer et al., 1993). The protocol utilized a two-step strategy that employed PCR with the *PfuUltra* high-fidelity DNA polymerase, and subsequent *Dpn*I digestion. Following transformation and selection of the mutant amplimers into XL10 Ultracompetent *Escherichia coli* cells (Stratagene, La Jolla, California), we controlled for polymerase fidelity by extracting plasmid DNA from many isolated bacterial clones and sequencing the L1 ORF of each clone to verify correct incorporation of nucleotide substitutions and the absence of spurious mutations elsewhere in the L1 ORF. Multiple mutant viral genomic clones containing correctly mutagenized sequences were isolated and utilized in subsequent experimentation. To create a full-length, HPV16(114/B) genome with a Cys428Ser substitution, the two complimentary oligonucleotides, forward 5′GTAACCCAGGCAATTGCTTCTCAAAAACATACACCTCC3′ and reverse 5′GGAGGTGTATGTTTTTGAGAAGCAATTGCCTGGGTTAC3′, were used with the change of G to C at nucleotide 6917. Cysteines were substituted for the most prevalent serine codon (TCT) in the HPV16(114/B) L1 ORF. To create a full-length, HPV16(114/B) genome with a Cys22Ser substitution, the two complimentary oligonucleotides, forward 5′CTACCCAACTTTATAAAACATCTAAACAGGCAGGTACATGTCC3′ and reverse 5′GGACATGTACCTGCCTGTTTAGATGTTTTATAAAGTTGGGTAG3′, were used with the change of GC to CT at nucleotide 4300. To create a full-length, HPV16(114/B) genome with a Cys28Ser substitution, the two complimentary oligonucleotides, forward 5′CAAACAGGCAGGTACATCTCCACCTGACATTATAC3′ and reverse 5′GTATAATGTCAGGTGGAGATGTACCTGCCTGTTTG3′, were used with the change of G to C at nucleotide 4318. To create a full-length, HPV16(114/B) genome with a Cys22,28Ser substitution, a full-length, HPV16(114/B) genome containing the Cys22Ser substitution, which was verified by sequencing, was utilized as a template and the two complimentary oligonucleotides, forward 5′CTAAACAGGCAGGTACATCTCCACCTGACATTATAC3′ and reverse 5′GTATAATGTCAGGTGGAGATGTACCTGCCTGTTTAG3′, were used with the change of GC to CT and G to C at nucleotides 4300 and 4318, respectively. Cysteines were substituted for the most prevalent serine codon (TCT) in the HPV16(114/B) L2 ORF.

Keratinocyte cultures and electroporation

Primary human foreskin keratinocytes (HFKs) were isolated from newborn circumcision as described previously (McLaughlin-Drubin et al., 2003). Briefly, keratinocytes were grown in 154 medium (Cascade Biologics, Inc., Portland, OR) supplemented with Human Keratinocyte Growth Supplement Kit (Cascade Biologics, Inc.). For electroporations, 30 μg of wild-type or mutant pBSHPV16(114/B) DNA was digested with *Bam*HI, linearizing the viral DNA at nucleotide 6151 in L1 and separating it from the vector sequence. Primary human foreskin keratinocytes (HFKs) were electroporated with the prepared DNA as described previously (McLaughlin-Drubin et al., 2003; Meyers et al., 1992). For mutant genomes, multiple clones obtained after mutagenesis were utilized to establish stable cell lines to control for PCR fidelity. Following electroporation, HPV16-positive cell lines were selected via immortalization as compared to HFKs that were mock transfected. Multiple stable cell lines were obtained for each wild-type and mutant construct.

Southern blot hybridization

Total cellular DNA was isolated as previously described (Meyers et al., 1992). Briefly, 5 μg of total cellular DNA was digested with *Bam*HI,

which linearizes the HPV16 genome. The samples were then separated by 0.8% agarose gel electrophoresis and transferred onto a GeneScreen Plus membrane (New England Nuclear Research Products, Boston, MA) as previously described (Smith, Campos, and Ozbun, 2007). Hybridization of the membrane utilized an HPV16-specific, whole genomic probe as previously described. (Meyers et al., 1992).

Organotypic "raft" cultures

Immortalized HFK lines which stably maintained wild-type and mutant episomal HPV16 DNA were grown in monolayer culture using E medium in the presence of mitomycin C-treated J2 3T3 feeder cells (Meyers et al., 1992). Raft tissues were grown as previously described (McLaughlin-Drubin and Meyers, 2005; McLaughlin-Drubin et al., 2003; Meyers et al., 1992). Briefly, HPV16-containing HFK lines were seeded onto rat tail type-1 collagen matrices containing J2 3T3 feeder cells not treated with mitomycin C. After epithelial attachment to the collagen matrices and growth to confluence, matrices were lifted onto stainless steel grids. Once lifted to the air–liquid interface, epithelial raft cultures were fed by diffusion from underneath with E medium, which lacked epidermal growth factor (EGF) and was supplemented with 20 mM 1,2-dioctanoyl-sn-glycerol (C8:0, Sigma Chemical, St. Louis, MO). Raft cultures were allowed to stratify and differentiate for 10, 15, and 20 days.

Histology and immunohistochemical staining

Raft cultures grown for 10 and 20 days were harvested, fixed in 10% neutral buffered formalin, and embedded in paraffin. Four-micrometer sections were cut and stained with hematoxylin and eosin as previously described (Meyers et al., 1992).

HPV isolation

For Optiprep fractionation, RT-PCR-, RT-qPCR-, and qPCR-based DNA encapsidation assays, 3-raft virus preps were prepared by dounce homogenization in 500 μl Benzonase buffer (0.05 M Na-phosphate [pH 8.0], 2 mM $MgCl_2$). Homogenizers were rinsed with 250 μl Benzonase buffer. 1 μl Benzonase (Sigma) was added to 499 μl of crude virus preps and incubated at 37 °C for 1 h. Then crude virus preps were brought to 1 M NaCl by adding 130 μl ice-cold 5 M NaCL. Crude virus preps were gently vortexed and then centrifuged at 4 °C for 10 min at 10,500 rpm in a microcentrifuge. Virus-containing supernatants were reserved as virus preps.

Optiprep purification of virions

Optiprep purification was performed as described previously (Buck et al., 2004; Gambhira et al., 2007). Briefly, 27%, 33%, 39% Optiprep gradients were produced by underlayering. Gradients were allowed to diffuse for 1 to 2 h at room temperature. Then 600 μl of clarified benzonase-treated virus preps were layered on top of the gradient. Tubes were then centrifuged in a SW55 rotor (Beckman) at 234,000×*g* for 3.5 h at 16 °C. After centrifugation, 11–500 μl fractions were carefully collected from the top of each tube.

Endpoint RT-PCR infectivity assays

The HPV16 infectivity studies were based on an in vitro system described by Smith et al. (1995) and White et al. (1998). HaCaT cells, an immortalized human keratinocyte cell line, which were kindly provided by N. Fusenig, were grown to confluence in Dulbecco's modified Eagle's medium supplemented with 10% fetal bovine serum, 2 mM glutamine, 1 mM pyruvate, 100 U/ml penicillin, and 100 μg/ml streptomycin and then seeded 50,000 cells/well in a 24-well plate. After 48 h, cells were subconfluent. The medium was aspirated from the HaCaT cells and Optiprep-fractionated CVPs were diluted either 1:20 for 10-day CVPs or 1:1000 for 20-day CVPs in HaCaT media and then inoculated to the HaCaTs in a total volume of 0.5 ml. One well on each plate received 0.5 ml of medium without virus as a negative control. The cells were incubated with the virus for 48 h at 37 °C. The ability to infect HaCaT cells after 48 h of incubation was determined by the presence of the spliced HPV16 E1^ E4 mRNA species (Smith et al., 1995 and White et al., 1998). mRNA was purified from the infected cells using the mRNA capture kit (Roche Molecular Biochemicals, Indianapolis, IN). Briefly, the medium was aspirated from the cells and the cells were washed two times with 0.5 ml ice cold 1× PBS. The final PBS wash was aspirated from the cells and 0.25 ml lysis buffer was added to each well. The cell lysates were removed from the wells and sonicated for 2 min in a cup horn sonicator on ice. Four microliters of 1:20 diluted biotinylated oligo dT was added to each lysate. The samples were incubated for 10 min at 42 °C. Fifty microliters of the lysate was transferred to a streptavidin-coated PCR tube and incubated for 3 min at 37 °C. The RNA captured in the tubes was washed three times with 200 μl of wash buffer and subsequently used in a RT reaction utilizing reagents from the First Strand cDNA kit (Roche Molecular Biochemicals). The cDNA was then used for nested PCR to detect the HPV16 E1E4 cDNA. Forty cycles of PCR was performed on the cDNA using 5′TGGAAGACCTGTTAATGGGCACA3′ as the forward primer (located at nucleotide position 797–820 in the HPV16 genome) and 5′ GTTACTATTACAGTTAATCCGTCC3′ (located at nucleotides 3584–3607 in the HPV16 genome) as the reverse primer. Ten percent of the first PCR mixture was used as template for 40 cycles of nested amplification utilizing 5′GGAATTGTGTGCCCCATCTGTTC3′ (located at nucleotide position 823–845 in the HPV16 genome) as the forward nested primer and 5′GCAACAACTTAGTGGTGTGGC3′ (located at nucleotide position 3507–3527 in the HPV16 genome) as the reverse nested primer. An additional set of primers specific for β-actin was included in the PCR mixture as a control for mRNA detection. The forward primer for the first reaction was 5′GAACCCCAAGGC-CAACCGCGA3′ and the reverse primer was 5′CCACACAGAG-TACTTGCGCTCAGG3′. The forward primer for the nested reaction was 5′GATGACCCAGATCATGTTTG3′ and the reverse primer was 5′GGAG-CATGATCTTGATCTTC3′. All PCR reactions contained 10 mM Tris–HCl, pH 8.3, 50 mM KCl, 2.5 mM $MgCl_2$, 200 μM dNTPs, 125 ng of each forward and reverse primer, and 2.5 U of Taq polymerase (Fisher Scientific). The temperature profile for the first reaction was 95 °C for 5 min, followed by 40 cycles of 95 °C for 30 s, 60 °C for 30 s, 72 °C for 1 min with a final 10-min extension at 72 °C. The temperature profile for the second reaction was 95 °C for 5 min, followed by 40 cycles of 95 °C for 30 s, 60 °C for 30 s, 72 °C for 30 s with a final 10-min extension at 72 °C. All PCR products were visualized by electrophoresis in a 2% agarose–ethidium bromide gel.

Quantitative RT-qPCR infectivity assays

As in the endpoint RT-PCR infectivity assay, HaCaT cells were grown to confluence in Dulbecco's modified Eagle's medium supplemented with 10% fetal bovine serum, 2 mM glutamine, 1 mM pyruvate, 100 U/ml penicillin, and 100 μg/ml streptomycin and seeded 50,000 cells/well in 24-well plates. CVPs were diluted with cell culture medium to a total volume of 0.5 ml. For neutralization assays, 1:100 dilutions of anti-P14/27 #2, anti-P56/75 #1, #S910-1, or RG-1 were added to the mixture above and incubated for 1 h at 37 °C prior to infection (Gambhira et al., 2007; Kondo et al., 2007). Medium was aspirated from HaCaT cells and 0.5 ml of diluted CVPs was added per well. One well on each plate received 0.5 ml of medium without virus as a negative control. The cells were incubated with the virus for 48 h at 37 °C. mRNA was harvested with the SurePrep TrueTotal RNA Purification Kit (Fisher Scientific). DNA contamination of columns was insignificant in that the optional on-column DNase-I treatment of extracted mRNA had no effect on downstream signal.

Amplification of both the viral target and endogenous cellular control target was performed using a duplex format in 0.2 ml, 96-well PCR plates (BIO-RAD) with a total reaction volume of 25 µl. All reactions containing RNAs from virus-infected cells were performed in duplicate or triplicate. Reverse transcription and quantitative PCR were performed in the same closed tube with approximately 250 ng of total RNA per reaction using the Quantitect Probe RT-PCR Kit (Qiagen). HPV16 E1^E4 primers used were the splice-site straddling, 5′GCTGATCCTGCAAGCAACGAAGTATC3′ (nt 868-3372) and 5′GGATTGGAGCACTGTCCACTGAG 3′ (nt 3535-3557) at final concentrations of 4 µM. A fluorogenic, dual-labeled, HPV16 E1^E4 probe of 5′ 6-FAM CACCGGAAACCCCTGCCACACCACTAAG BHQ-1 3′ (nt 3493-3520) was utilized at a final concentration of 0.2 µM to detect E1^E4 cDNA. Primers and probe were developed using Gene Link Software: OligoAnalyzer 1.2, and OligoExplorer 1.2. TATA-binding protein (TBP) amplicons were created using primers 5′ CACGGCACTGATTTTCAGTTCT 3′ (nt 627-648) and 5′ TTCTTGCTGCCAGTCTGGACT 3′ (nt 706-686) at final concentrations of 0.125 µM. TBP amplicons were detected by the fluorogenic TaqManTM probe 5′HEX TGTGCACAGGAGCCAAGAGTGAAGA BHQ-13′ used at 0.2 µM. TBP primer sequences were obtained from those previously described (Culp and Christensen, 2003). All primers were synthesized by Integrated DNA Technologies (Coralville, IA). All QRT-PCR reactions were performed using the iQ5 (BIO-RAD). Cycling conditions were 50 °C for 30 min (reverse transcription) and 95 °C for 15 min, followed by 42 cycles of 94 °C for 15 s and 54.5 °C for 1 min. Amplification efficiencies of each primer set was 93% for E1^E4 and 97% for TBP. Relative quantities of viral target cDNA were determined using REST software.

qPCR-based DNA encapsidation assay

To detect endonuclease-resistant genomes in crude virus preps or Optiprep fractions, only benzonase-treated virus preps were utilized so that all non-encapsidated genomes were digested. To break up any aggregated virions within samples, virus preps and fractions were sonicated utilizing a Misonix 3000 sonicator for 30 s at a power setting of 6.5. To release all encapsidated viral genomes, 10 µl sonicated virus prep or 20 µl Optiprep fraction was added to 2 µl Proteinase K, 10 µl 10% SDS, 2 µl pCMV-GFP (140 ng/µl) carrier DNA, and brought up to 200 µl with Hirt buffer. Tubes were rotated at 37 °C for 2 h. Tubes were spiked with 12 µl 2-Mercaptoethanol, vortexed for 30 s, and followed by 10 min of incubation in boiling water. Immediately, an equal amount of phenol–chloroform–isoamyl alcohol (25:24:1) was added and the mixture was extracted for the aqueous phase. An equal amount of chloroform was added and again extracted for the aqueous phase. DNA was EtOH precipitated overnight at −20 °C. After centrifugation, the DNA pellet was washed with 70% EtOH and resuspended in 20 µl TE overnight and was termed an endonuclease-resistant viral genome prep. To detect viral genomes in the endonuclease-resistant viral genome preps, a Qiagen Quantitect SYBR Green PCR kit was utilized. Amplification of the viral target was performed in 0.2 ml, 96-well PCR plates (BIO-RAD) with a total reaction volume of 25 µl. l µl of each endonuclease-resistant viral genome prep was analyzed in triplicate for each independent experiment. Amplification of HPV16 genomes was performed using 0.3 µM 5′CCATATAGACTATTGGAAACACATGCGCC3′ as the forward primer (nt 2839–2868) and 0.3 µM 5′CGTTAGTTGCAGTTCAATTGCTTGTAATGC3′ as the reverse primer (nt 2960–2989). Oligonucleotides were synthesized by Integrated DNA Technologies (Coralville, IA). A standard curve was generated by amplifying 1 µl aliquots of 10^4, 10^3, 10^2, and 10^1 serially diluted pBSHPV16 copy number controls. Acceptable R^2 values for standard curves were at or above 0.99. A Bio-Rad iQ5 Multicolor Real-Time qPCR machine and software were utilized for PCR amplifications and subsequent data analysis. The PCR thermocycling profile was as follows: 15-min hot-start at 95 °C, followed by 40 cycles at 15 s at 94 °C, 30 s at 52 °C, and 30 s at 72 °C. Data analysis commenced during the extension phase. Melt curve analyses were performed for all SYBR Green PCR amplifications to verify specificity of the reaction. Melt curves and first derivative melt curves were run immediately after the last PCR cycle. Melt curves were produced by plotting the fluorescence intensity against temperature as the temperature was increased from 60 to 95 °C at 0.5 °C/s. To further verify specificity of the reaction, qPCR products were visualized via gel electrophoresis for single products of expected size. Calculation of the exact number of endonuclease-resistant viral genomes per 3-raft virus prep was determined by comparing experimental values to the number of actual pBSHPV16 copies within the serially diluted copy number controls.

Acknowledgments

We thank Tadahito Kanda, Kazunari Kondo, and Richard Roden for access to their anti-L2 antibodies; Horng Shen Chen and Tim Culp for assistance with qPCR; and the Meyers' laboratory for critical reading of this manuscript. This work was supported by a PHS Grant from the NIAID (R01AI57988).

References

Bordeaux, J., Forte, S., Harding, E., Darshan, M.S., Klucevsek, K., Moroianu, J., 2006. The l2 minor capsid protein of low-risk human papillomavirus type 11 interacts with host nuclear import receptors and viral DNA. J. Virol. 80 (16), 8259–8262.
Bossis, I., Roden, R.B., Gambhira, R., Yang, R., Tagaya, M., Howley, P.M., Meneses, P.I., 2005. Interaction of tSNARE syntaxin 18 with the papillomavirus minor capsid protein mediates infection. J. Virol. 79 (11), 6723–6731.
Buck, C.B., Pastrana, D.V., Lowy, D.R., Schiller, J.T., 2004. Efficient intracellular assembly of papillomaviral vectors. J. Virol. 78 (2), 751–757.
Buck, C.B., Thompson, C.D., Pang, Y.Y., Lowy, D.R., Schiller, J.T., 2005. Maturation of papillomavirus capsids. J. Virol. 79 (5), 2839–2846.
Buck, C.B., Cheng, N., Thompson, C.D., Lowy, D.R., Steven, A.C., Schiller, J.T., Trus, B.L., 2008. Arrangement of L2 within the papillomavirus capsid. J. Virol.
Campos, S.K., Ozbun, M.A., 2009. Two highly conserved cysteine residues in HPV16 L2 form an intramolecular disulfide bond and are critical for infectivity in human keratinocytes. PLoS ONE 4 (2), e4463.
Chen, X.S., Garcea, R.L., Goldberg, I., Casini, G., Harrison, S.C., 2000. Structure of small virus-like particles assembled from the L1 protein of human papillomavirus 16. Mol. Cell 5 (3), 557–567.
Conway, M.J., Alam, S., Ryndock, E.J., Cruz, L., Christensen, N.D., Roden, R.B.S., Meyers, C., in press. Tissue-spanning redox gradient-dependent assembly of native HPV16 virions. J. Virol.
Conway, M.J., Meyers, C., 2009. Replication and assembly of human papillomaviruses. J. Dental Res. 88 (4), 307–317.
Culp, T.D., Christensen, N.D., 2003. Quantitative RT-PCR assay for HPV infection in cultured cells. J. Virol. Methods 111 (2), 135–144.
Day, P.M., Baker, C.C., Lowy, D.R., Schiller, J.T., 2004. Establishment of papillomavirus infection is enhanced by promyelocytic leukemia protein (PML) expression. Proc. Natl. Acad. Sci. U.S.A. 101 (39), 14252–14257.
Day, P.M., Gambhira, R., Roden, R.B., Lowy, D.R., Schiller, J.T., 2008a. Mechanisms of human papillomavirus type 16 neutralization by l2 cross-neutralizing and l1 type-specific antibodies. J. Virol. 82 (9), 4638–4646.
Day, P.M., Lowy, D.R., Schiller, J.T., 2008b. Heparan sulfate-independent cell binding and infection with furin-precleaved papillomavirus capsids. J. Virol. 82 (24), 12565–12568.
Doorbar, J., 2005. The papillomavirus life cycle. J. Clin. Virol. 32 (Suppl. 1), S7–S15.
Doorbar, J., Gallimore, P.H., 1987. Identification of proteins encoded by the L1 and L2 open reading frames of human papillomavirus 1a. J. Virol. 61 (9), 2793–2799.
Finnen, R.L., Erickson, K.D., Chen, X.S., Garcea, R.L., 2003. Interactions between papillomavirus L1 and L2 capsid proteins. J. Virol. 77 (8), 4818–4826.
Gambhira, R., Karanam, B., Jagu, S., Roberts, J.N., Buck, C.B., Bossis, I., Alphs, H., Culp, T., Christensen, N.D., Roden, R.B., 2007. A protective and broadly cross-neutralizing epitope of human papillomavirus L2. J. Virol. 81 (24), 13927–13931.
Holmgren, S.C., Patterson, N.A., Ozbun, M.A., Lambert, P.F., 2005. The minor capsid protein L2 contributes to two steps in the human papillomavirus type 31 life cycle. J. Virol. 79 (7), 3938–3948.
Ishii, Y., Tanaka, K., Kanda, T., 2003. Mutational analysis of human papillomavirus type 16 major capsid protein L1: the cysteines affecting the intermolecular bonding and structure of L1-capsids. Virology 308 (1), 128–136.
Ishii, Y., Ozaki, S., Tanaka, K., Kanda, T., 2005. Human papillomavirus 16 minor capsid protein L2 helps capsomeres assemble independently of intercapsomeric disulfide bonding. Virus Genes 31 (3), 321–328.
Kirnbauer, R., Taub, J., Greenstone, H., Roden, R., Durst, M., Gissmann, L., Lowy, D.R., Schiller, J.T., 1993. Efficient self-assembly of human papillomavirus type 16 L1 and L1-L2 into virus-like particles. J. Virol. 67 (12), 6929–6936.
Kondo, K., Ishii, Y., Ochi, H., Matsumoto, T., Yoshikawa, H., Kanda, T., 2007. Neutralization of HPV16, 18, 31, and 58 pseudovirions with antisera induced by

immunizing rabbits with synthetic peptides representing segments of the HPV16 minor capsid protein L2 surface region. Virology 358 (2), 266–272.
Li, M., Beard, P., Estes, P.A., Lyon, M.K., Garcea, R.L., 1998. Intercapsomeric disulfide bonds in papillomavirus assembly and disassembly. J. Virol. 72 (3), 2160–2167.
Liu, W.J., Gissmann, L., Sun, X.Y., Kanjanahaluethai, A., Muller, M., Doorbar, J., Zhou, J., 1997. Sequence close to the N-terminus of L2 protein is displayed on the surface of bovine papillomavirus type 1 virions. Virology 227 (2), 474–483.
Longworth, M.S., Laimins, L.A., 2004. Pathogenesis of human papillomaviruses in differentiating epithelia. Microbiol. Mol. Biol. Rev. 68 (2), 362–372.
Lowe, J., Panda, D., Rose, S., Jensen, T., Hughes, W.A., Tso, F.Y., Angeletti, P.C., 2008. Evolutionary and structural analyses of alpha-papillomavirus capsid proteins yields novel insights into L2 structure and interaction with L1. Virol. J. 5 (1), 150.
Mach, H., Volkin, D.B., Troutman, R.D., Wang, B., Luo, Z., Jansen, K.U., Shi, L., 2006. Disassembly and reassembly of yeast-derived recombinant human papillomavirus virus-like particles (HPV VLPs). J. Pharm. Sci. 95 (10), 2195–2206.
McLaughlin-Drubin, M.E., Meyers, C., 2005. Propagation of infectious, high-risk HPV in organotypic "raft" culture. Methods Mol. Med. 119, 171–186.
McLaughlin-Drubin, M.E., Wilson, S., Mullikin, B., Suzich, J., Meyers, C., 2003. Human papillomavirus type 45 propagation, infection, and neutralization. Virology 312 (1), 1–7.
McLaughlin-Drubin, M.E., Christensen, N.D., Meyers, C., 2004. Propagation, infection, and neutralization of authentic HPV16 virus. Virology 322 (2), 213–219.
Meyers, C., Frattini, M.G., Hudson, J.B., Laimins, L.A., 1992. Biosynthesis of human papillomavirus from a continuous cell line upon epithelial differentiation. Science 257 (5072), 971–973.
Meyers, C., Mayer, T.J., Ozbun, M.A., 1997. Synthesis of infectious human papillomavirus type 18 in differentiating epithelium transfected with viral DNA. J. Virol. 71 (10), 7381–7386.
Pyeon, D., Lambert, P.F., Ahlquist, P., 2005. Production of infectious human papillomavirus independently of viral replication and epithelial cell differentiation. Proc. Natl. Acad. Sci. U.S.A. 102 (26), 9311–9316.
Richards, R.M., Lowy, D.R., Schiller, J.T., Day, P.M., 2006. Cleavage of the papillomavirus minor capsid protein, L2, at a furin consensus site is necessary for infection. Proc. Natl. Acad. Sci. U.S.A. 103 (5), 1522–1527.
Sapp, M., Fligge, C., Petzak, I., Harris, J.R., Streeck, R.E., 1998. Papillomavirus assembly requires trimerization of the major capsid protein by disulfides between two highly conserved cysteines. J. Virol. 72 (7), 6186–6189.
Smith, L.H., Foster, C., Hitchcock, M.E., Leiserowitz, G.S., Hall, K., Isseroff, R., Christensen, N.D., Kreider, J.W., 1995. Titration of HPV-11 infectivity and antibody neutralization can be measured in vitro. J. Investig. Dermatol. 105, 438–444.
Smith, J.L., Campos, S.K., Ozbun, M.A., 2007. Human papillomavirus type 31 uses a caveolin 1- and dynamin 2-mediated entry pathway for infection of human keratinocytes. J. Virol. 81 (18), 9922–9931.
Touze, A., Mahe, D., El Mehdaoui, S., Dupuy, C., Combita-Rojas, A.L., Bousarghin, L., Sizaret, P.Y., Coursaget, P., 2000. The nine C-terminal amino acids of the major capsid protein of the human papillomavirus type 16 are essential for DNA binding and gene transfer capacity. FEMS Microbiol. Lett. 189 (1), 121–127.
Trus, B.L., Roden, R.B., Greenstone, H.L., Vrhel, M., Schiller, J.T., Booy, F.P., 1997. Novel structural features of bovine papillomavirus capsid revealed by a three-dimensional reconstruction to 9 A resolution. Nat. Struct. Biol. 4 (5), 413–420.
Wang, H.K., Duffy, A.A., Broker, T.R., Chow, L.T., 2009. Robust production and passaging of infectious HPV in squamous epithelium of primary human keratinocytes. Genes Dev. 23 (2), 181–194.
White, W.I., Wilson, S.D., Bonnez, W., Rose, R.C., Koenig, S., Suzich, J.A., 1998. In vitro infection and type-restricted antibody-mediated neutralization of authentic human papillomavirus type 16. J. Virol. 72 (2), 959–964.
Yang, R., Day, P.M., Yutzy, W.H.t., Lin, K.Y., Hung, C.F., Roden, R.B., 2003. Cell surface-binding motifs of L2 that facilitate papillomavirus infection. J. Virol. 77 (6), 3531–3541.
Zhou, J., Sun, X.Y., Louis, K., Frazer, I.H., 1994. Interaction of human papillomavirus (HPV) type 16 capsid proteins with HPV DNA requires an intact L2 N-terminal sequence. J. Virol. 68 (2), 619–625.